BULLETIN OF THE POLISH ACADEMY OF SCIENCES
TECHNICAL SCIENCES, Vol. 63, No. 1, 2015
DOI: 10.1515/bpasts-2015-0026

Azimuth ambiguity suppression in SAR images using Doppler-sensitive signals

Cz. LEŚNIK*, P. SERAFIN, and A. KAWALEC

Institute of Radioelectronics, Faculty of Electronics, Military University of Technology, 2 S. Kaliskiego St., 00-908 Warsaw, Poland

Abstract. In the article the problem of the azimuth ambiguity in synthetic aperture radar (SAR) images and its genesis are presented. A method of suppressing the ambiguities by utilization of Doppler-sensitive signals is proposed, and the necessary modifications to the SAR synthesis algorithm are discussed. The SAR system parameters required for an optimal performance of the method are discussed and simulation results are presented.

Key words: Synthetic Aperture Radar (SAR), azimuth ambiguity, Doppler-sensitive signals.

1. Introduction

Synthetic aperture radar (SAR) techniques [1–5] allow to obtain very high resolution radar images of the observed objects due to the coherent integration of the echo signals collected over a long distance called the synthetic aperture (SA).

Developers of SAR systems, as it is in the case of any radar system for air surveillance, must acknowledge the limitations that result from the very nature of the radar signals and the propagation of the electromagnetic waves. One of such limitations is the sounding frequency (pulse repetition frequency – PRF) criterion that affects the ambiguity of the SAR image in the direction parallel to the radar carrier trajectory (azimuth or Cross-Range direction).

When too low a PRF is applied, the initial echo signal phase change may be greater than 2π, which results in false (ambiguous) images of observed objects [6, 7].

The literature presents various methods of elimination those ambiguities in SAR images where properties of the real antenna were exploited [6], the image synthesis algorithm was modified [7] or multichannel reception was applied [8]. In this paper a method of ambiguity suppression with application of Doppler-sensitive signals as sounding signals in SAR systems is presented. As this requires some modifications to the image synthesis algorithm, those are described as well.

2. The origin of the azimuth ambiguities

The SAR system principle is based on terrain observation by a moving radar along its route, storing the received echo signals and processing them as if they were received by a single, very long antenna [1–5].

In order to present the SAR echo signal structure a side-looking configuration airborne radar will be considered. The geometry of such a system is shown in Fig. 1.

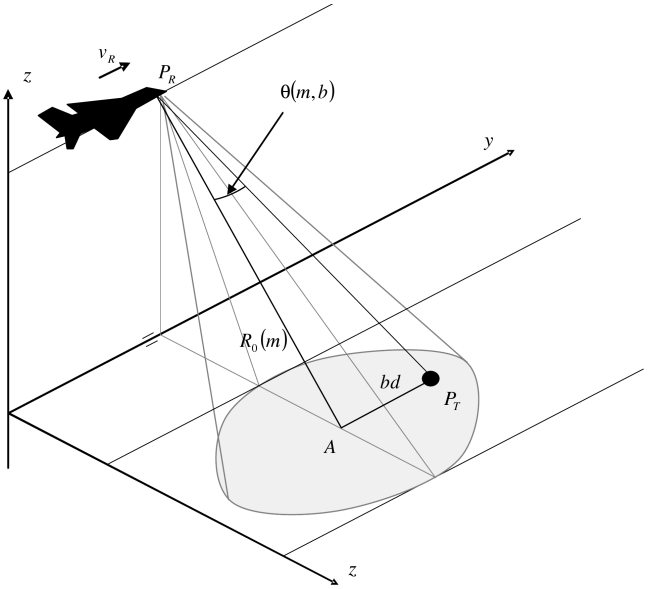

Fig. 1. The geometry of the described system

A radar sensor mounted on board of an aircraft is moving with a constant velocity v_R, at a constant altitude h_R, along a straight route, parallel to the OY axis. The radar is emitting sounding signals at a carrier frequency f_0, with a PRF equal to F_p.

Directional pattern of the real antenna is positioned so its main beam is perpendicular to the velocity vector and illuminates a patch of terrain.

Echo signals reflected from objects in illuminated space are received and stored in the systems memory.

In a synthetic aperture radar, the distance between radar and the observed target changes due to the motion of the radar platform (or the target). If a coordinate system from Fig. 1 is assumed, then, from the geometry of the system shown in Fig. 1, one could describe the distance change function in the following form

*e-mail: Czeslaw.Lesnik@wat.edu.pl

$$R_T(u) = \sqrt{x_T^2 + (y_T - v_R u)^2 + (z_T - h_R)^2}, \quad (1)$$

where u is the time associated with radar movement and is called the "slow time", in contrast to the time t associated with electromagnetic wave propagation and called the "fast time", (x_T, y_T, z_T) are the coordinates of the observed target positioned on the ground.

For the analytic form of the sounding signal presented as follows [4]

$$s_T(t) = a(t)\exp(j2\pi f_0 t), \quad (2)$$

where $a(t)$ is the complex amplitude of the signal, and f_0 is its carrier frequency, the received echo signal from a single point-like object can written down in the following form [4]

$$s_R(t,u) = a\left[t - t_T(u)\right]\exp\left\{j2\pi f_0\left[t - t_T(u)\right]\right\}, \quad (3)$$

where t_T is the time from the moment of the transmission of the sounding signal to the return of the echo signal and it is defined as follows [1, 4]

$$t_T(u) = \frac{2R_T(u)}{c}. \quad (4)$$

In the radar receiver the echo signals are down-converted, then, taking into account (4), the echo signal can be written as

$$\begin{aligned} s_{RDC}(t,u) &= A\left[t - t_T(u)\right]\exp\left[-j2\pi f_0 t_T(u)\right] \\ &= u\left[t - \frac{2R_T(u)}{c}\right]\exp\left[-j2\pi\frac{2R_T(u)}{\lambda}\right]. \end{aligned} \quad (5)$$

Due to the fact, that the radar starts sending the sounding signals from discrete positions along its trajectory, the received signals are naturally sampled in the slow time (azimuth) direction. Moreover in order to store and process the signals in a digital signal processing system they have to be sampled in the fast time domain.

The received signals are stored in a two-dimensional array, where one dimension represents the fast time, and the other – number of the sounding period, associated with the slow time. Then the echo signal from (5) can be written as follows [1, 4]

$$\begin{aligned} s_{RDC}(m,n) = u\left[mt_s - \frac{2R_T(n)}{c}\right]\exp \\ \cdot\left[-j2\pi\frac{2R_T(n)}{\lambda}\right], \end{aligned} \quad (6)$$

where m is the number of the range cell (number of a fast-time sample), t_s is the sampling period, n is the slow-time sample number and $R_T(n)$ can be defined as follows

$$R_T(n) = \sqrt{x_T^2 + (y_T + nd)^2 + h_R^2}. \quad (7)$$

In Fig. 2. a 2-D distribution of the magnitude of the raw echo signal from a single point-like object is presented.

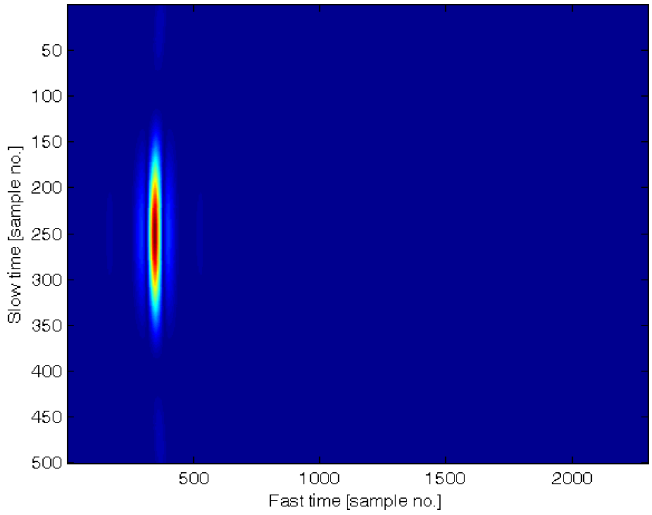

Fig. 2. Two-dimensional amplitude distribution of a simulated raw echo signal form a single point like object

In Eq. (7) d is the distance between two consecutive points along the radar trajectory, where the sounding signal is emitted, and it can be computed as follows [1]

$$d = \frac{v_R}{F_p}. \quad (8)$$

The initial phase of the echo signals is proportional to the distance to the object and changes in a hyperbolic way. One has to notice, that this phenomenon is in fact a result of the Doppler effect, and the instantaneous frequency $f_D(u)$ of the raw echo signal from a single object in the azimuth domain is equal to the Doppler shift of the signal spectrum. It is easy to observe that the raw echo SAR signal is a chirp with a nearly linear frequency modulation. In Fig. 3. such a signal and its spectrogram are presented.

Due to its discrete nature, the SAR signal has the same limitations to its spectrum as any sampled signal, and therefore it should satisfy the Nyquist criterion.

In order to meet the Nyquist criterion in the fast time domain, a proper value of the sampling frequency f_s has to be established.

In the slow time domain, the signal is sampled in consecutive sounding periods. The selection of a proper value of the pulse repetition frequency (PRF) F_p in SAR has to meet at least two requirements [2]. The first one concerns the range of the observed distances, the increase of which requires the reduction of the PRF. The second one is in fact the Nyquist criterion, which means that the PRF should be at least twice the frequency of the highest Doppler component existing in the echo signal.

In Figs. 2 and 3 one can observe the amplitude modulation of the signal in azimuth domain with the real antenna pattern, which is the limiting factor for the raw signal Doppler bandwidth. The effective width of the Doppler band B_D is strongly dependent on the radar velocity v_R and the width of the main lobe of the real antenna pattern $\theta_{\max}$ according to the following equation [1]

$$B_D = 4\frac{v_R}{\lambda}\sin\frac{\theta_{\max}}{2} \approx 2\frac{v_R}{\lambda}\sin\theta_{\max}, \tag{9}$$

where λ is the wavelength of the sounding signal, and the main lobe width $\theta_{\max}$ is its width at the -3 dB level.

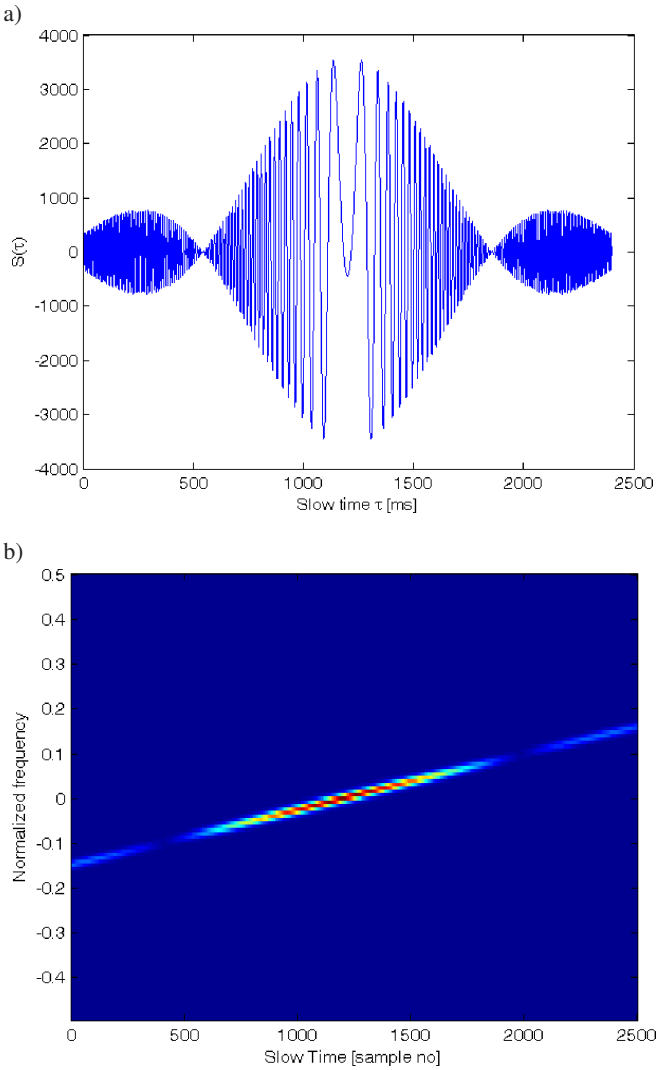

Fig. 3. The real part of the raw SAR signal – cross-section in azimuth domain (a), and the spectrogram of the raw SAR signal (b)

If a PRF value lowers than the $2B_D$ is chosen, the superimposing of the adjacent periods of the spectrum (aliasing) will occur. As a result, there will be additional (false) points where the f_D reaches zero. At those points the SAR image synthesis algorithm will generate replicas of the object image, which makes the SAR image ambiguous and severely degenerates its quality.

In Fig. 4. an example of the SAR raw signal in azimuth direction with Nyquist criterion violation and its spectrogram is presented. As in Fig. 3. amplitude modulation with antenna pattern is visible, but in this case the points where the frequency of the signal reaches zero are observable within the main beam.

In Fig. 5. a comparison of SAR images generated with simulated signals for the two above described cases are presented. Due to the aliasing phenomenon additional, ambiguous, object images, also referred to as ghost targets, occur in the plot.

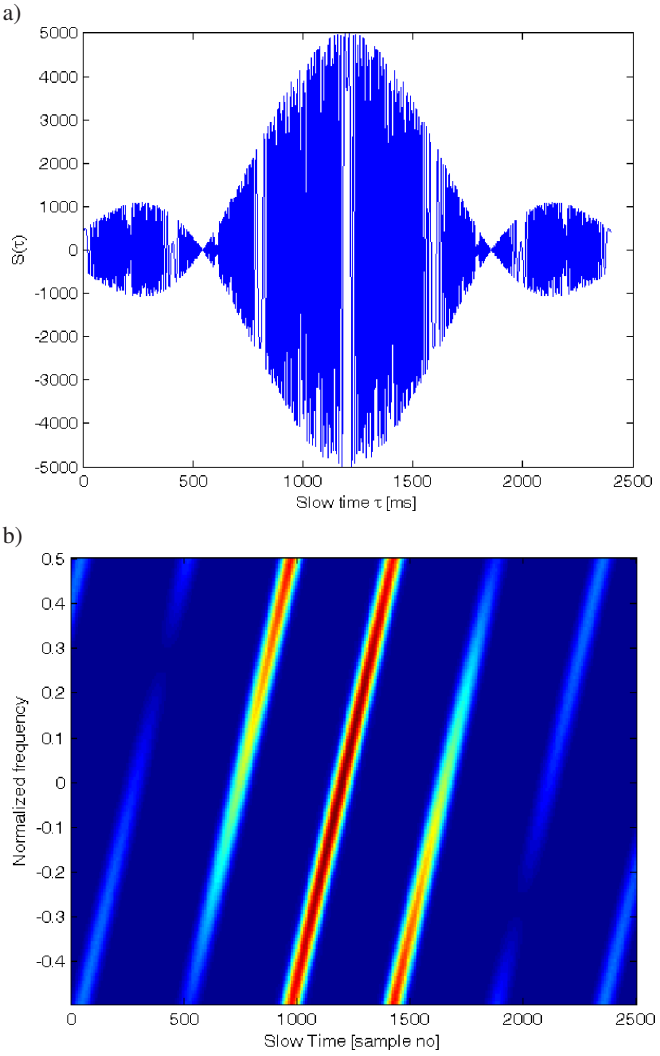

Fig. 4. Real part of the raw SAR signal – cross-section in azimuth domain (a), and spectrogram of the raw SAR signal with the Nyquist criterion violated (b)

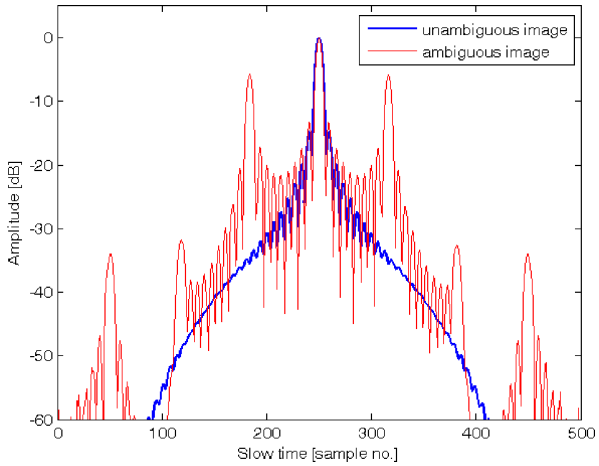

Fig. 5. A comparison of an unambiguous and ambiguous SAR images

The most natural approach to this problem would be the reduction of the beamwidth $\theta_{\max}$ of the real antenna, which allows to suppress the ambiguities, but at the price of image azimuth resolution due to the signal history shortening.

Another way of avoiding the ambiguity problem, if a compromise between a range and Doppler requirements cannot be found, is to narrow the swath in the range direction, however this reduces the amount of information acquired by the system.

From the above considerations, it appears that the optimal situation would be if, during synthesis of a particular pixel of the SAR image, the history of the signal was long enough to achieve the required azimuth resolution, but at the same time the contributions from neighboring objects had the negligibly low amplitude.

Those contradictory requirements can be met by application of Doppler-sensitive sounding signals.

3. Doppler-sensitive signals

The idea to employ the signals sensitivity to Doppler effect has been considered earlier for both domains of active sonar to eliminate the reverberations [9] as well as in air surveillance radar to solve the Doppler ambiguity for high velocity targets with linear range migration [10]. In this work the Doppler sensitivity defined as the matched filter output signal amplitude reduction rate is considered, which allows to separate the targets in SAR signal, thus suppressing the azimuth ambiguities.

The most popular tool for evaluation of the radar signals is their Woodward's ambiguity function. This function describes a complex envelope of the signal at the output of the optimal receiver against the echo delay time τ and its Doppler shift f_D. Usually it is defined as [11–14]

$$|\chi(\tau, f_D)| = \left| \int_{-\infty}^{\infty} u(t)\, u*(t+\tau) \exp(j2\pi f_D t)\, dt \right| \quad \text{for} \quad |\tau| \le T, \tag{10}$$

where $u(t)$ – complex envelope of the signal, $u*(t)$ – complex conjugate of $u(t)$, τ – time delay, f_D – Doppler frequency shift, T – signal duration time.

This function possesses many interesting properties. From the discussed problems point of view the most essential are that:

- the ambiguity function has its maximum in the origin of the coordinate system, which means, that the signal reaches maximal value only if the signal if fully matched to the filter,
- the width of ambiguity function around the origin define the potential simultaneous resolution in time (range) and Doppler (radial velocity),
- the cross-section of the ambiguity function with the $\chi\tau$ plane (from (10), for $f_D = 0$)

$$|\chi(\tau, 0)| = \left| \int_{-\infty}^{\infty} u(t) u*(t+\tau) dt \right| \tag{11}$$

is the magnitude of the one-dimensional autocorrelation function of the complex envelope of the signal,

- the cross-section of the ambiguity function with the χf_D plane (from (10), for $\tau = 0$)

$$|\chi(0, f_D)| = \left| \int_{-\infty}^{\infty} |u(tt)|^2 \exp(-j2\pi f_D t) dt \right| \tag{12}$$

is the magnitude of the Fourier transform of the squared magnitude of the complex envelope of the signal.

In practical situations the real envelope of the signal (magnitude of the complex envelope) is close to rectangular. Then the function (12) takes a shape of a $|\sin c\, x|$ – like function with the first zero for $f_D = 1/T$. Probably the most commonly used radar signal, a chirp with linear frequency modulation (LFM) has the ambiguity function described as follows [12]

$$|\chi(\tau, f_D)| = \left| \left(1 - \frac{|\tau|}{T}\right) \frac{\sin\left[\pi T \left(1 - \frac{|\tau|}{T}\right)\left(f_D + \frac{B}{T}\tau\right)\right]}{\pi T \left(1 - \frac{|\tau|}{T}\right)\left(f_D + \frac{B}{T}\tau\right)} \right| \quad \text{for} \quad |\tau| \le T, \tag{13}$$

where B – is the signal bandwidth (LFM sweep width).

The cross-section of the function (13) with the χf_D (for $\tau = 0$) plane takes the form

$$|\chi(0, f_D)| = \left| \frac{\sin(\pi T f_D)}{\pi T f_D} \right|,$$

which does not mean, however, that the signal level at the output of the optimal receiver reaches its first zero for $f_D = 1/T$. The Doppler shift of the signal spectrum causes a dislocation of the signal maximum along the time axis according to the rule $\tau = -(f_D/B)\, T$, with a simultaneous reduction of the maximum signal value [12]

$$\chi_{\max}(f_D) = 1 - \frac{|f_D|}{B}. \tag{14}$$

From the above equation, for $f_D = 1/T$ the LFM signal level at the output of the optimal receiver will not be zero, but it will be slightly reduced and the maximum of the signal will be shifted in time. This phenomenon, called the "Range-Doppler Coupling", is responsible for a most desirable in air surveillance radars Doppler tolerance of this kind of signals.

In this article, however, we are looking for signals with low Doppler tolerance or high Doppler sensitivity, where this sensitivity can be expressed as the width of the main lobe of the $\chi_{\max}(f_D)$. An example of a class of such signals are the binary phase shift keying (BPSK) signals. It is possible to show that the maximum of the main lobe of the signal at the output of the optimal receiver as a function of the Doppler shift is given by [15]

$$|\chi_{\max}(f_D)| = \frac{1}{N} \left| \frac{\sin(\pi f_D N t_{chip})}{\sin(\pi f_D t_{chip})} \right|, \tag{15}$$

where t_{chip} is the duration time of a single chip (a segment of the signal), N is the code length (number of chips). The first zero of this function is located at $f_D = 1/(N\, t_{chip})$.

As a representative of the BPSK signals a pseudo noise (PN) binary phase manipulated signal has been considered. A general form of the complex envelope of the PN signal (assuming unitary amplitude) can be described as [11]

$$u(t) = \begin{cases} \sum_{n=0}^{N-1} \text{rect}\left[\frac{t-(0.5+n)t_{chip}}{t_{chip}}\right] e^{j\theta_n} & \\ \qquad\qquad \text{for } 0 \le t < Nt_{chip} & \\ 0 \qquad\qquad \text{for } 0 > t \ge Nt_{chip} & \end{cases}, \tag{16}$$

where n – chip number, θ_n – initial phase of the n-th chip of the signal, $\theta_n \in \{0, \pi\}$.

rect(t) – unitary amplitude rectangular pulse with unitary duration time

$$\text{rect}(t) = \begin{cases} 1 & \text{for } -0.5 \le t < 0.5 \\ 0 & \text{for } -0.5 > t \ge 0.5 \end{cases}.$$

The ambiguity function of a PN signal with the code length $N = 255$is presented in Fig. 6.

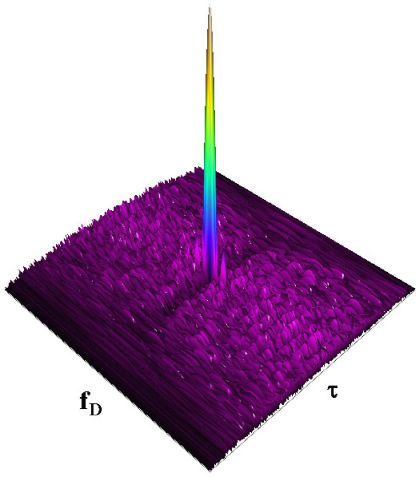

Fig. 6. Ambiguity function for a PN signal with the code length $N = 255$

4. Application of Doppler-sensitive signals to SAR

If a signals with a sufficient level of Doppler sensitivity is applied as the sounding signal in SAR, the amplitude of the raw echo signal after the range compression will depend not only on the real antenna pattern, but also on the effect of compression filter mismatch. This means that the amplitude of the signal may be reduced in order to shorten the signal history, but it can also be restored for the synthesis of the appropriate point of the SAR image.

This restoration of the signals amplitude is done through a proper shift of the matched filter transfer function in the frequency domain by the exact value of the Doppler frequency.

From the previous paragraph the width of the ambiguity function of the PN-BPSK signal in the Doppler shift direction is equal to $2/T$. This means that in order to suppress the ambiguities, the sounding signal duration time should be close to a pulse repetition interval, which suggests that the radar should work in a continuous wave regime. If this is the case the first zero of the ambiguity function along the Doppler axis will fall close to the first ambiguity (see Fig. 7).

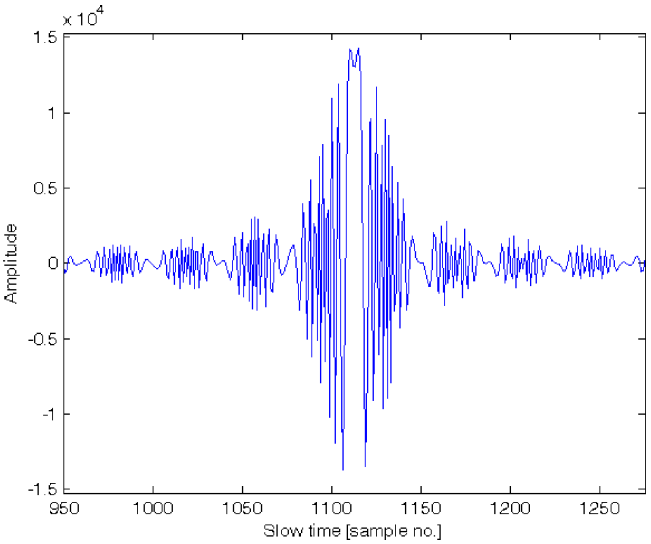

Fig. 7. Real part of the range-compressed raw SAR signal. The first zero of the ambiguity function falls exactly at $f_D = PRF$

One has to notice that in a single sounding period the radar receives the echo signals from a large number of objects from different azimuth angles, thus having different Doppler shifts. The compensation, however, can be performed only for a single object, which allows to distinguish its echo signal and suppress signals form other objects. Therefore in order to employ the sensitivity of the signals to the Doppler effect, a SAR synthesis algorithm, where range compression as well as the azimuth compression are performed for each slow time sample separately, must be applied. This can be done by the exact two-dimensional time domain correlation algorithm [16].

This algorithm, without the Doppler effect compensation, bases on the range-compressed raw SAR signal and performs convolution of samples of the signal with the reference function chosen according to the range cell migration function. It can be described as follows [16]

$$G_{SAR}(m,n) = \sum_{b=-N_{SA}/2}^{N_{SA}/2} s_{RC} \cdot [l(m,b), n+b]\, w_{ref}(b), \tag{17}$$

where $G_{SAR}(m,n)$ is the complex intensity of a SAR image pixel for m-th range cell and n-th azimuth position, $s_{RC}(m,n)$ is the (m,n)-th sample of the raw SAR signal after the range compression, $w_{ref}(b)$ is the azimuth reference function for the b-th synthetic aperture element, and b is an integer number from range of $(-N_{SA}/2; N_{SA}/2)$, N_{SA} being the number of synthetic aperture elements.

In Eq. (17) $l(m,b)$ is the number of the range cell computed form the range cell migration compensation (RCMC) function

$$l(m,b) = \left\lfloor \frac{\sqrt{R_0^2(m) + b^2 d^2} - R_{\min}}{dR} \right\rfloor, \tag{18}$$

where $\lfloor x \rfloor$ is the floor function returning the greatest integer function not greater than x, and dR is the range cell size associated with the sampling frequency f_s [4]

$$dR = \frac{c}{2f_s}. \tag{19}$$

In the above equation c is the electromagnetic wave propagation velocity.

By $R_0(m)$ the distance between the radar trajectory and the target from m-th range cell equal to

$$R_0(m) = mdR + R_{\min}, \tag{20}$$

where $R_{\min}$ is the distance associated with the first range cell.

The modified algorithm also performs the sum form Eq. (17), however the signal being convolved with the reference function is changed. It is range-compressed in a Doppler-compensated matched filter according to the number of the synthetic aperture element for which it is computed. Then the algorithm Eq. (17) takes the following form

$$G_{SAR\,\mathrm{mod}}(m,n) = \sum_{b=-N_{SA}/2}^{N_{SA}/2} s_{RC}^b \cdot [l(m,b), n+b]\, w_{ref}(b), \tag{21}$$

where $s_{RC}^b\,[l(m,b), k+b]$ is a sample of the raw SAR signal for $(k+b)$-th pulse (azimuth position) and for $m(l,b)$ range cell after range compression in the matched filter compensated by a Doppler shift associated with b-th synthetic aperture element. This signal can be computed as follows

$$s_{RC}^b(m, n+b) = \sum_{p=0}^{N_p} s_{RDC} \cdot (m+p, n+b) w_{MF}(m+p) \exp\left[-j2\pi\, f_D(m,b)\right], \tag{22}$$

where $s_{RDC}(m,n)$ is the m-th fast time sample of the down-converted raw signal before the range compression for the n-th azimuth position, $w_{MF}(m+p)$ is $(m+p)$-th sample of the fast time matched filter pulse response, $f_D(m,b)$ is the value of the Doppler shift of the raw signal for the b-th synthetic aperture element and the m-th range cell. This frequency depends on the immediate value of the radial velocity of the observed object relative to the radar antenna, and for subsequent SA elements it changes with the sinus of the angle of observation $\theta(m,b)$

$$f_D(m,b) = 4\frac{v_R}{\lambda} \sin\theta(m,b). \tag{23}$$

From the $\Delta P_R P_T A$ triangle (see Fig. 1) having catheti equal to $R_0(m)$ and $d \cdot b$ one can obtain

$$\sin\theta(m,b) = \frac{R_0(m)}{\sqrt{R_0^2(m) + d^2 b^2}}. \tag{24}$$

The above considerations have been verified by computer simulations. Echo signals from point-like objects received by a SAR system have been modeled. The most important parameters of the simulation are presented in Table 1.

Table 1

No.	Parameter	Value
1	Carrier frequency f_0	15 GHz
2	PRI	3.6 ms
3	Pulse duration time T_i	0.45–3.4 ms
4	SAR platform velocity	50 m/s

The simulations were conducted for both LFM and PN-BPSK signals. The ambiguity performance of the SAR system was measured as a ratio between the peak of the ambiguous and true image (AASR – Azimuth Ambiguity to Signal Ratio).

In Fig. 8. a comparison of azimuth cross-sections of SAR images synthesized from LFM (uncorrected) and PN-BPSK (corrected) signals is presented. An ambiguity suppression grater than 20 dB has been achieved due to the signal Doppler sensitivity.

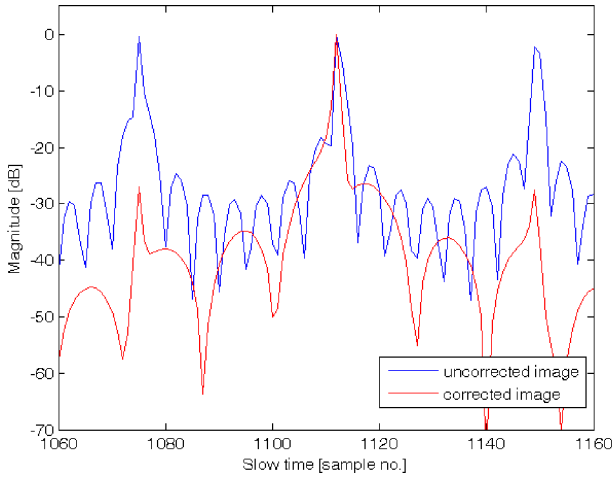

Fig. 8. A comparison of SAR images (azimuth cross-sections) for LFM (blue) and Doppler-corrected PN-BPSK (red) signals

In Fig. 9. AASR against signal duration time normalized to PRI for different synthetic aperture lengths is presented.

Selecting the CW regime for a SAR radar allows for a significant reduction of ambiguous images, with AASR as good as -30 dB.

The question of the practical application of the proposed method raises the issues of non-ideal radar's carrier movement, in particular the problem of the carrier's velocity instability. This, in the case of drastic velocity fluctuations, could impair the performance of the matched filter tuning procedure and, consequently, the SAR image restoration. It should be noted, however, that in order to achieve a high resolution SAR image the carrier's movement parameters must be estimated, either by an additional on-board navigation system or through the autofocus procedures. Therefore the velocity of the carrier would be known with a sufficient accuracy to perform the filter tuning.

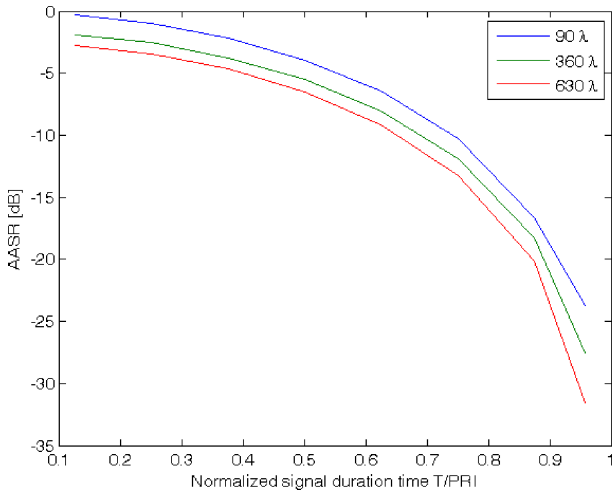

Fig. 9. The AASR against normalized signal duration time for different synthetic aperture lengths

5. Conclusions

In this article a method of azimuth ambiguities suppression in SAR images has been presented. The proposed method is based on utilizing the signals sensitivity to the Doppler effect. Radar systems using Doppler-sensitive signals present a significant reduction of the signal at the output of the matched filter due to the Doppler shift of the received echo, which shortens the raw signal history and suppresses the amplitude of ambiguous images. In order to achieve the desired SAR image azimuth resolution the signal history is reconstructed by adaptation of the matched filter during the image synthesis algorithm.

The simulation results show that better than 30 dB ambiguity reduction can be obtained for a CW radar.

REFERENCES

[1] B.C Wang, *Digital Signal Processing Techniques and Applications in Radar Image processing*, John Wiley & Sons, Inc., New Jersey, 2008.

[2] I.G. Cumming and F.H. Wong, *Digital Processing of Synthetic Aperture Radar Data. Algorithms and Implementation*, Artech House, Boston/London 2005.

[3] B. Dawidowicz, A. Gados, A. Gorzelanczyk, A. Jarzebska, K.S. Kulpa, M. Mordzonek, P. Samczynski, and M. Smolarczyk, "First Polish SAR trials", *IEE Proc. Radar, Sonar and Navigation* 153 (2), 135–143 (2006).

[4] M. Skolnik, *Radar Handbook*, third edition, McGraw-Hill Book Company, New York, 2008.

[5] D. Massonnet and J.C. Souyris, *Imaging with Synthetic Aperture Radar*, CRC Press, New York, 2008.

[6] K.D. Rolt and H. Schmidt, "Azimuthal ambiguities in synthetic aperture sonar and synthetic aperture radar imagery", *IEEE J. Oceanic Engineering* 17 (1), 73–79 (1992).

[7] A. Moreira, "Suppressing the Azimuth Ambiguities in Synthetic Aperture Radar Images", *IEEE Trans. on Geoscience and Remote Sensing* 31 (4), 885–895, (1993).

[8] X. Ma, Z. Sun, Z. Dong, and H. Huang, "Azimuth ambiguity of multi-channel SAR", *IEEE Int. Geoscience and Remote Sensing Symposium (IGARSS)* 3, 3807–3810 (2012).

[9] T. Collins and P. Atkins, "Doppler-sensitive active sonar pulse designs for reverberation processing", *IEE Proc. Radar, Sonar and Navigation* 145 (6), 347–353 (1998).

[10] R.F. Tigrek, W.J.A. de Heij, and P. van Genderen, "Solving Doppler ambiguity by Doppler sensitive pulse compression using multi-carrier waveform", *Eur. Radar Conf. EuRAD* 1, 72–75 (2008).

[11] C.E. Cook and M. Bernfeld, *Radar Signals. An Introduction to Theory and Application*, Artech House, Boston, 1993.

[12] N. Levanon and E. Mozeson, *Radar Signals*, John Wiley & Sons, New Jersey, 2004.

[13] M.A. Richards, J.A. Scheer, and W.A. Holm, *Principles of Modern Radar. Vol. I: Basic Principles*, SciTech Publishing, Raleigh, 2010.

[14] M.A. Richards, *Fundamentals of Radar Signal Processing, Second Edition*, McGraw-Hill Education, New York, USA, 2014.

[15] Jing Liu, Huichang Zhao, and Yanping Zhu, "The ambiguity function of pn-chirp pulse signal", *Int. Conf. on Information Science and Technology* 1, 543–547 (2011).

[16] R. Bamler, "A comparison of range-Doppler and wavenumber domain SAR focusing algorithms", *IEEE Trans. on Geoscience and Remote Sensing* 30 (4), 706–713 (1992).